Immunology
The Journal of cells, molecules, systems and technologies

British Society for immunology

IMMUNOLOGY ORIGINAL ARTICLE

Neuroprotective role of fibroblast growth factor-2 in experimental autoimmune encephalomyelitis

Andrea Rottlaender, Hannah Villwock, Klaus Addicks and Stefanie Kuerten

Department of Anatomy I, University of Cologne, Cologne, Germany

doi:10.1111/j.1365-2567.2011.03450.x
Received 5 February 2011; revised 4 April 2011; accepted 7 April 2011.
A.R. and H.V. contributed equally to this work.
Correspondence: Dr S. Kuerten, Department of Anatomy I, University of Cologne, Joseph-Stelzmann-Str. 9, 50931 Cologne, Germany.
Email: stefanie.kuerten@uk-koeln.de
Senior author: Dr S. Kuerten

Summary

The role of fibroblast growth factor-2 (FGF-2) in multiple sclerosis and its animal model experimental autoimmune encephalomyelitis is discussed. This study is the first to use FGF-2$^{-/-}$ mice to further address the involvement of FGF-2 in the disease process. We demonstrate that immunization with myelin oligodendrocyte glycoprotein peptide 35–55 induces more severe experimental autoimmune encephalomyelitis in FGF-2$^{-/-}$ mice compared with FGF-2$^{+/+}$ mice. The antigen-specific cytokine response to myelin oligodendrocyte glycoprotein peptide and the degree of central nervous system inflammation was similar in both groups. However, FGF-2$^{-/-}$ mice displayed increased infiltration of CD8^{+} T cells and macrophages/microglia. In addition, nerve fibre degeneration and axonal loss were augmented, whereas the extent of remyelination in central nervous system lesions was reduced. FGF-2 has been associated with the induction of demyelination and the inhibition of myelin production by oligodendrocytes. Our study supports the opposing notion that FGF-2 can also assert a neuroprotective function. This may be particularly appealing when it comes to targeting the neurodegenerative aspect of multiple sclerosis.

Keywords: demyelination; experimental autoimmune encephalomyelitis; fibroblast growth factor-2; multiple sclerosis; neuroprotection; remyelination

Introduction

Multiple sclerosis (MS) is an autoimmune disorder of the central nervous system (CNS). Despite intensive research, the aetiology of the disease remains controversial. Therapeutic strategies are mainly aimed at reducing the inflammatory processes of the disease but they are not efficient in long-term prevention of neurodegeneration.[1]

The role of growth factors in MS is attracting increasing attention. In particular the fibroblast growth factor 2 (FGF-2) has been subject to discussion. FGF-2 is one of 19 subtypes of the FGF family and was first described in 1975.[2] It is expressed in a multitude of tissues, acting in a pleiotropic and multifunctional way.[3] As a result of its capability to inhibit neuronal cell apoptosis while being a mitogenic factor for neuronal progenitors and supporting the differentiation and regeneration of various cell types,[4–9] it appears to be a promising therapeutic agent when considering the neurodegenerative aspect of MS. Studies in experimental autoimmune encephalomyelitis (EAE), the common animal model for MS, supported a beneficial role of FGF-2 in the pathogenesis of the disease. Intrathecal injection of a herpes simplex virus type-1 replication defective multigene vector, engineered with the human FGF-2 gene, significantly inhibited the clinicopathological signs of myelin oligodendrocyte glycoprotein (MOG) peptide 35–55-induced EAE.[10] In that study, mice showed a significant reduction in the numbers of myelin-toxic cells with a consecutive increase in myelin-producing oligodendrocytes and oligodendrocyte precursors in the proximity of demyelinated lesions. In support of these data Messersmith *et al.*[11] found that FGF-2 mRNA peaked during the initial stage of remyelination, suggesting a directly regulating impact on oligodendrocyte

Abbreviations: BDNF, brain-derived neurotrophic factor; CNS, central nervous system; EAE, experimental autoimmune encephalomyelitis; FGF, fibroblast growth factor; H&E, haematoxylin & eosin; MOG, myelin oligodendrocyte glycoprotein; MS, multiple sclerosis.

lineage cell responses in addition to paracrine or autocrine effects on astrocytes.

However, there are also studies reporting contradictory data. On the one hand, the inhibition of myelin production by oligodendrocytes upon activation of the FGF receptor has been demonstrated.[12] On the other hand, increased FGF-2 levels were capable of triggering demyelination in the adult rat brain[13] and the actual lack of FGF-2 was associated with oligodendrocyte regeneration in another study.[14] In addition, levels of FGF-2 have been shown to be elevated in the cerebrospinal fluid of patients with MS. This elevation was particularly evident in patients with MS experiencing a clinical relapse, and subsequently showing only unsatisfactory recovery.[15] Overall, a correlation between the rise of FGF-2 levels in the cerebrospinal fluid and more aggressive demyelination and less efficient remyelination was suggested.[15]

The present study is the first to make use of FGF-$2^{-/-}$ mice to further investigate the role of FGF-2 in EAE. Disease was induced with MOG peptide 35–55 in FGF-$2^{-/-}$ and FGF-$2^{+/+}$ mice and the subsequent development of clinical EAE, the peripheral immune response to MOG peptide and CNS histopathology in the acute and chronic stage of the disease were evaluated. Our data indicate that FGF-2 acts as a neuroprotective agent in MOG peptide-induced EAE – being associated with the prevention of nerve fibre degeneration/axonal loss while promoting remyelination in CNS lesions.

Materials and methods

Mice

Female FGF-$2^{-/-}$ and wild-type FGF-$2^{+/+}$ mice (6–8 weeks old were obtained from the Jackson Laboratory (Bar Harbor, ME). The mice were maintained on the C57BL/6 background at our local animal facilities. The mice had been generated by a targeted deletion replacing a 0·5-kb portion of the *FGF-2* gene, including 121 bp of the promoter and the entire first exon, with an *Hprt* minigene.[16] The genotype of each mouse was confirmed by PCR according to the protocol provided by the Jackson Laboratory. All treatments complied with the institutional guidelines.

Induction and clinical assessment of EAE

The MOG peptide 35–55 was obtained from EZBiolab (Carmel, IN). Incomplete Freund's adjuvant was prepared as a 1 : 9 mixture of mannide monooleate (Sigma-Aldrich, St Louis, MO) and paraffin oil (EMScience, Gibbstown, NJ), complete Freund's adjuvant (CFA) was obtained by mixing *Mycobacterium tuberculosis* H37 RA (Difco Laboratories, Franklin Lakes, NJ) at 5 mg/ml into incomplete Freund's adjuvant. Mice were immunized subcutaneously in both sides of the flank with a total dose of 100 μg MOG peptide emulsified in CFA. Pertussis toxin (List Biological Laboratories, Hornby, ON, Canada) was given at 200 ng per mouse on the day of immunization and 48 hr later. Clinical assessment of EAE was performed daily according to the standard EAE scale: (0), no disease; (1), floppy tail; (2), hind limb weakness; (3), full hind limb paralysis; (4), quadriplegia; (5), death. Mice that were in between the clear-cut gradations of clinical signs were scored intermediate in increments of 0·5.

ELISPOT assays

ImmunoSpot M200 plates (Cellular Technology Limited, Cleveland, OH) were coated overnight with the capture antibodies in sterile PBS (100 μl per well). AN-18 (eBioscience, San Diego, CA) was used at 3 μg/ml for capturing interferon-γ (IFN-γ) and TC-11-18H10 (BD Pharmingen, San Diego, CA) was used at 4 μg/ml for interleukin-17 (IL-17). The plates were blocked for 2 hr at room temperature with sterile PBS containing 1% BSA (Sigma-Aldrich). The cells were suspended in HL-1 cell culture medium (Lonza, Cologne, Germany) supplemented with 1 mM L-glutamine (Sigma-Aldrich). The cells were plated in the absence (medium control) or presence of antigen (final concentration of 15 μg/ml MOG peptide 35–55). Either 10^6 spleen cells or 5×10^5 draining lymph node cells were plated per well, respectively. The plates were cultured at 37° and 7% CO_2 for 24 hr. Consecutively, the detection antibodies were added for overnight incubation, all diluted in sterile PBS containing 1% BSA and 0·025% Tween-20. FITC-labelled rat anti-mouse R4-6A2 (purified and FITC-labelled in our laboratory) was used at 0·5 μg/ml for detecting IFN-γ, and rat anti-mouse TC11-8H4.1-biotin for IL-17 (0·5 μg/ml). As a third reagent for IFN-γ anti-FITC-AP (Dako, Glostrup, Denmark) was added at 1 : 500 dilution in PBS containing 1% BSA and 0·025% Tween-20, Streptavidin-AP (DakoCytomation) was added at 1 : 1000 for IL-17. After incubation for 2 hr at room temperature plates were developed using nitroblue tetrazolium/5-bromo-4-chloro-3-indolyl phosphatase substrate (Kirkegaard and Perry Laboratories, Gaitherburg, MD) for 10–30 min. The resulting spots were counted on an ImmunoSpot Series 5 Analyzer (Cellular Technology Limited).

Assessment of CNS infiltration

At the peak of acute EAE and on day 90 after EAE induction when clinical scores had reached a stable plateau (chronic EAE), mice were killed by CO_2 asphyxiation. The spinal cord was removed and snap-frozen in liquid nitrogen. Seven-micrometer thick longitudinal frozen sections were cut on a Reichert-Jung Cryocut CM1850 cryostat (Leica, Wetzlar, Germany) and mounted on SUPERFROST/Plus slides (Carl Roth, Karlsruhe, Germany). Five

equidistant longitudinal sections per mouse were stained with haematoxylin & eosin (H&E) according to the standard protocol. Images were obtained using a Zeiss Axiophot microscope (Zeiss, Göttingen, Germany) connected to a LM digital camera system (Universal Imaging Corporation Ltd., Marlow, UK). The images covered the entire white matter on each section including the inflammatory infiltrates if present. The area of white matter and infiltrates was measured using ZEISS AXIOVISION software.

Immunohistochemistry was performed on five 7-μm thick equidistant longitudinal spinal cord sections from each mouse. Designated sections were air-dried for 2 hr at room temperature. Sections were incubated with the primary antibodies (all from eBioscience) at 1 : 500 dilution in PBS/1% BSA for 1 hr at room temperature. Rat anti-mouse GK1.5 was used for the detection of $CD4^+$ T cells, rat anti-mouse 53-6.7 for $CD8^+$ T cells, rat anti-mouse RA3-6B2 for B cells, rat anti-mouse BM8 for macrophages/microglia and rat anti-mouse RB6-8C5 for granulocytes. Sections were then incubated with goat anti-rat biotinylated antibody (Dako) at 1 : 400 dilution in PBS/1%BSA for 30 min at room temperature, followed by incubation with Neutravidin-Dylight 549 (Thermo Fisher Scientific, Rockford, IL) at 1 : 300 dilution for 30 min at room temperature. Hoechst solution (bisbenzimide H; Sigma, St Louis, MO) was used at 1 : 1000 dilution for nuclear staining. Sections were covered with Aqua-Poly/Mount coverslips (Polysciences, Warrington, PA). Specificity controls included the omission of primary and secondary antibodies. The potency and reactivity of each monoclonal antibody were regularly checked by testing on sections of mouse spleen tissue. Sections were observed with a Zeiss Axioskop 50 epifluorescence microscope. For fluorescence analysis a 'rhodamine' filter (Nr. 15 of Carl Zeiss, excitation BP 546/12, beamsplitter FT 580, emission LP 590) and an 'ultraviolet' filter (Nr. 1 of Carl Zeiss, excitation BP 365/12, Emission LP 397) were used. Digital images of CNS infiltrates were acquired using a slow scan CCD camera (SPOT RT; Diagnostic Instruments, Sterling Heights, MI) and software. The acquisition software IMAGEPRO PLUS (Media Cybernetics, Silver Spring, MD) was used for consecutive image analysis.

Electron microscopy

To investigate the degree of CNS degeneration/regeneration and axonal loss, mice were perfused intracardially with 4% paraformaldehyde/4% glutaraldehyde in 0·1 M PBS in the chronic stage of EAE (day 90 after immunization). The tissue was post-fixed at 4° for at least 24 hr. Spinal cords were carefully removed from the vertebral canal. The lumbar part was separated and divided into three equally thick segments. The tissue was rinsed in cacodylate buffer three times and treated with 1% uranyl acetate in 70% ethanol for contrast enhancement. Subsequently, the tissue was dehydrated in a graded ethanol series and specimens were embedded in epon (Serva Electrophoresis GmbH, Heidelberg, Germany). Eighty-nanometre thick ultrathin sections of each plastic-embedded spinal cord sample were cut on an ultramicrotome (Reichert, Bensheim, Germany). Swimming in the water trough of the diamond knife, the ultrathin sections were stretched with xylene vapour and thereafter carefully suspended on 150 mesh hexagonal Formvar-coated copper grids (Electron Microscopy Sciences, Hatfield, PA). The preparations were stained with 1% aqueous uranyl acetate solution for 20 min and Reynold's lead citrate solution for 7 min. Sections were examined with a Zeiss EM 902A transmission electron microscope at 80 kV acceleration voltage and images were taken with an electron microscope digital camera system (MegaView, analysis© docu 3.2; Olympus Soft Imaging Systems GmbH, Münster, Germany). In each individual mouse the images obtained covered the whole spinal cord lesional area that was evident on the sections. The spinal cord lesions were located in each of the three lumbar spinal cord samples, resulting in approximately 30 images per mouse. The examination of all histopathology was performed by an observer blinded as to the sensitization and clinical status of the animals.

Statistical analysis

SIGMASTAT software (Version 7.0; SPSS, Chicago, IL) was used to assess the statistical significance of the differences between two groups. Analysis of variance was chosen for the analysis of the differences in clinical disease. Student's *t*-test was used for calculating the significance of the differences in antigen-specific cytokine secretion, lesion sizes, nerve fibre numbers and degeneration/regeneration. Statistical significance was set at $P \leq 0{\cdot}05$.

Results

Clinical disease is augmented in FGF-$2^{-/-}$ mice

The FGF-$2^{-/-}$ mice ($n = 10$) and FGF-$2^{+/+}$ mice ($n = 8$) were immunized with MOG peptide 35–55 in CFA according to the disease-inducing protocol. Mice were evaluated daily for the occurrence of clinical symptoms of EAE. The disease outcome in both groups is depicted in Fig. 1 encompassing a period of 90 days post-immunization. Both FGF-$2^{-/-}$ and FGF-$2^{+/+}$ mice showed chronic non-remitting EAE, which was, however, augmented in the former. The disease incidence was 100% in both groups of mice. The disease onset was on day 16·11 ± 8·10 in FGF-$2^{-/-}$ mice compared with day 16·25 ± 3·03 in FGF-$2^{+/+}$ mice ($P = 0{\cdot}730$). The mean maximal score in the acute stage of the disease was 2·25 ± 0·71 in FGF-$2^{-/-}$ mice compared with 2·13 ± 1·02 in FGF-$2^{+/+}$ mice ($P = 0{\cdot}794$). The difference in the severity of clinical EAE pertained to the chronic stage of the disease, which was

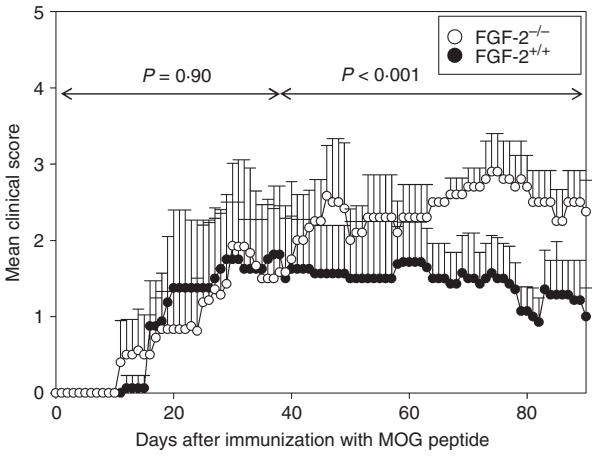

Figure 1. Fibroblast growth factor-2-deficient (FGF-$2^{-/-}$) mice display more severe myelin oligodendrocyte glycoprotein (MOG) peptide-induced experimental autoimmune encephalomyelitis than wild-type mice. FGF-$2^{-/-}$ and FGF-$2^{+/+}$ mice were immunized subcutaneously with MOG peptide in complete Freund's adjuvant. Pertussis toxin was given on days 0 and 2 after immunization. Mice were scored daily for the occurrence of clinical symptoms according to the standard scale. Results for FGF-$2^{-/-}$ mice (n = 10) mice are plotted in black and for FGF-$2^{+/+}$ mice (n = 8) in white and are representative for three independent experiments. Mean values + SD are shown.

entered around day 40 after immunization. Here, the mean maximal score was 3·00 ± 0·58 in FGF-$2^{-/-}$ versus 1·63 ± 0·65 in FGF-$2^{+/+}$ mice ($P < 0·001$).

There are no differences in the antigen-specific peripheral immune response in FGF-$2^{-/-}$ and FGF-$2^{+/+}$ mice

To test whether the differences in clinical EAE reflected differences in the peripheral immune response to MOG peptide, we evaluated the magnitude of the antigen-specific IFN-γ or IL-17 response by ELISPOT, testing spleen and draining lymph node cells from FGF-$2^{-/-}$ and FGF-$2^{+/+}$ mice on day 10 after immunization. Results are displayed in Fig. 2 and refer to n = 8 mice per group. The data show that the MOG 35–55-specific IFN-γ (Fig. 2a) and IL-17 (Fig. 2b) response was similar in FGF-$2^{-/-}$ and FGF-$2^{+/+}$ mice and in both compartments tested. Representative images are given in Fig. 2(c).

The extent of CNS inflammation is similar in FGF-$2^{-/-}$ and FGF-$2^{+/+}$ mice

The degree of inflammation was evaluated by measuring the size of spinal cord inflammatory lesions in relation to the total spinal cord white matter on H&E-stained sections from FGF-$2^{-/-}$ and FGF-$2^{+/+}$ mice. The data are shown in Fig. 3. At the peak of acute EAE, spinal cord histopathology was characterized by extensive cellular infiltration in the white matter (Fig. 3a–c). In FGF-$2^{-/-}$

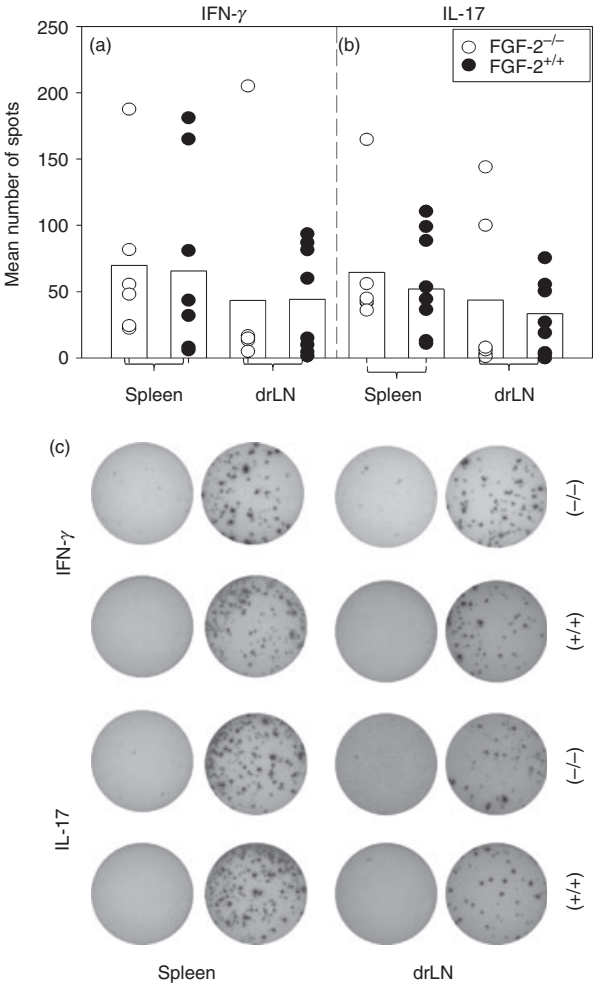

Figure 2. The myelin oligodendrocyte glycoprotein (MOG):35–55-specific interferon-γ (IFN-γ)/interleukin-17 (IL-17) response is similar in fibroblast growth factor-2-deficient (FGF-$2^{-/-}$) and FGF-$2^{+/+}$ mice. FGF-$2^{-/-}$ (n = 8) and FGF-$2^{+/+}$ mice (n = 8) were immunized with MOG peptide 35–55. On day 10 after immunization spleen and draining lymph nodes were removed. ELISPOT assays were performed, measuring the antigen-specific IFN-γ (a) and IL-17 (b) response. White dots refer to FGF-$2^{-/-}$ mice, black dots refer to FGF-$2^{+/+}$ mice. The bars delineate the mean value for each group. (c) Representative images for both groups of mice and both compartments. The results are representative for three independent experiments.

mice (n = 6) 5·3 ± 4·1% of the white matter was infiltrated, compared with 4·4 ± 3·1% in FGF-$2^{+/+}$ mice (n = 6). The difference did not reach statistical significance (P = 0·474). As we have described before,[17] in chronic EAE CNS histopathology is characterized by increasing demyelination and axonal damage, whereas the number of infiltrating cells decreases. Three months after immunization, aggregated infiltrating cells were absent in both FGF-$2^{-/-}$ and FGF-$2^{+/+}$ mice, only a few disseminated cells were found in the tissue (Fig. 3d–f). Overall, lesions accounted for 0·18 ± 0·38% of spinal cord white

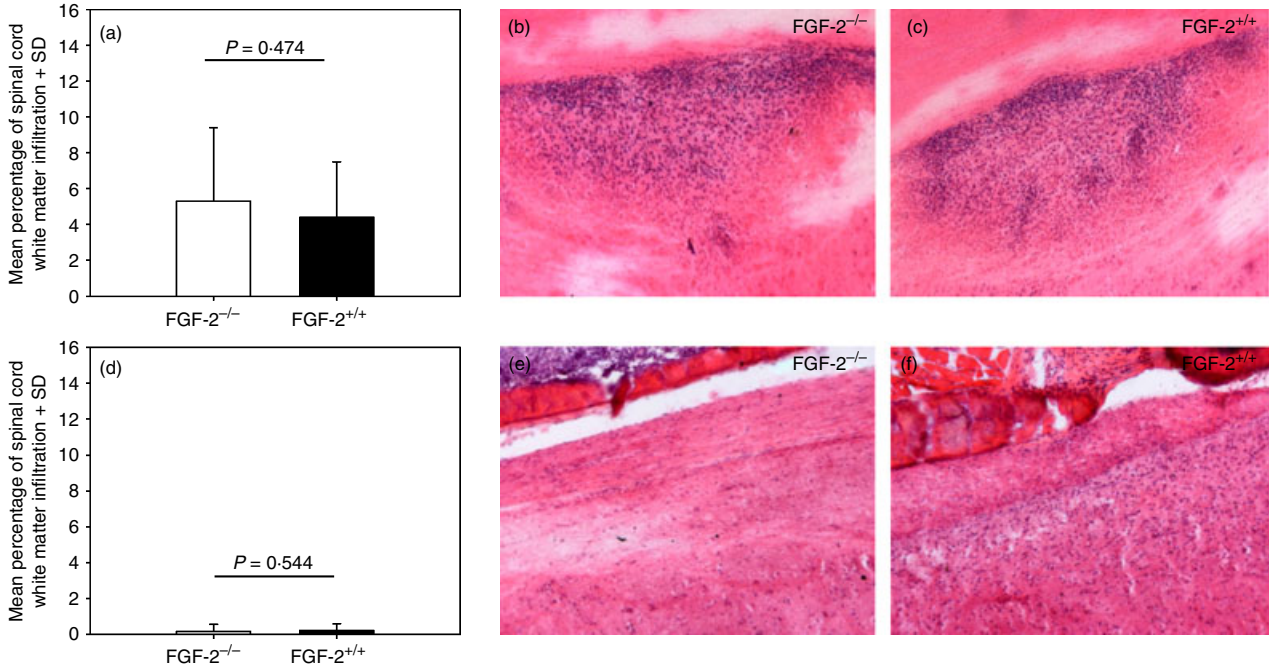

Figure 3. The degree of central nervous system (CNS) infiltration is similar in fibroblast growth factor-2-deficient (FGF-$2^{-/-}$) and FGF-$2^{+/+}$ mice. The magnitude of CNS infiltration was studied at the peak of acute (a–c) experimental autoimmune encephalomyelitis (EAE) and in chronic (d–f) EAE in FGF-$2^{-/-}$ ($n = 6$) (a–c) and FGF-$2^{+/+}$ ($n = 6$) (d–f) mice. (a, d) Percentage of spinal cord white matter infiltration in acute and chronic EAE. White bars refer to FGF-$2^{-/-}$ mice, black bars to FGF-$2^{+/+}$ mice. Results are expressed as means + SD. (b, c, e, f) and are representative of three independent experiments. Representative images are at 100× magnification. H&E staining.

matter in FGF-$2^{-/-}$ mice ($n = 6$) and 0·22 ± 0·38% in FGF-$2^{+/+}$ mice ($n = 6$) ($P = 0·544$) in the chronic stage of the disease.

CNS lesion composition differs in FGF-$2^{-/-}$ and FGF-$2^{+/+}$ mice

Next to evaluating the extent of spinal cord inflammation we also assessed the lesion composition at the peak of disease in FGF-$2^{-/-}$ and FGF-$2^{+/+}$ mice. The numbers of $CD4^+$ (Fig. 4a–c) and $CD8^+$ (Fig. 4d–f) T cells, B cells (Fig. 4g–i), macrophages/microglia (Fig. 4j–l) and granulocytes (Fig. 4m–o) per mm^2 are shown. There was no difference in the number of infiltrating $CD4^+$ T cells ($P = 0·186$), B cells ($P = 0·164$) and granulocytes ($P = 0·785$). However, significantly more $CD8^+$ T cells ($P < 0·001$) and macrophages/microglial cells ($P < 0·001$) were found in spinal cord lesions of FGF-$2^{-/-}$ compared with FGF-$2^{+/+}$ mice.

CNS degeneration is increased and regeneration is reduced in FGF-$2^{-/-}$ compared with FGF-$2^{+/+}$ mice

It has been reported that FGF-2 induces an increase in the number of oligodendrocyte precursors and of myelin-forming oligodendrocytes, which are the major source of remyelinating cells, in areas of demyelination and axonal loss. To investigate whether FGF-2 may play a neuroprotective role in MOG peptide-induced EAE, we evaluated the degree of nerve fibre degeneration and regeneration in FGF-$2^{-/-}$ and FGF-$2^{+/+}$ mice. For the assessment of myelin pathology, the *g*-ratio was calculated for each individual nerve fibre by dividing the axonal diameter by the total nerve fibre diameter.[18] The *g*-ratio reflects that myelin sheath thickness increases concomitantly with axon diameter, maintaining a relatively stable quotient.[19,20] A *g*-ratio between 0·60 and 0·75 is considered to be optimal for conduction of the action current.[21] In the present study, fibres with a *g*-ratio < 0·60 were considered as dysmyelinating/demyelinating. In addition, axonal pathology was assessed, taking into account mitochondrial size, the presence of increased inner tongues, the nearest neighbour neurofilament diameter and axolysis. Fibres that showed either myelin or axonal pathology or both were counted as 'dystrophic'. Fibres with a *g*-ratio > 0·75 were considered as remyelinated. In each image, the total number of nerve fibres was evaluated and compared in FGF-$2^{-/-}$ and FGF-$2^{+/+}$ mice. The degree of degeneration and regeneration in the mice is expressed in %, relating to the total number of nerve fibres (Fig. 5).

In FGF-$2^{-/-}$ mice 62·44 ± 3·14% of all nerve fibres within CNS lesions were classified as dystrophic in

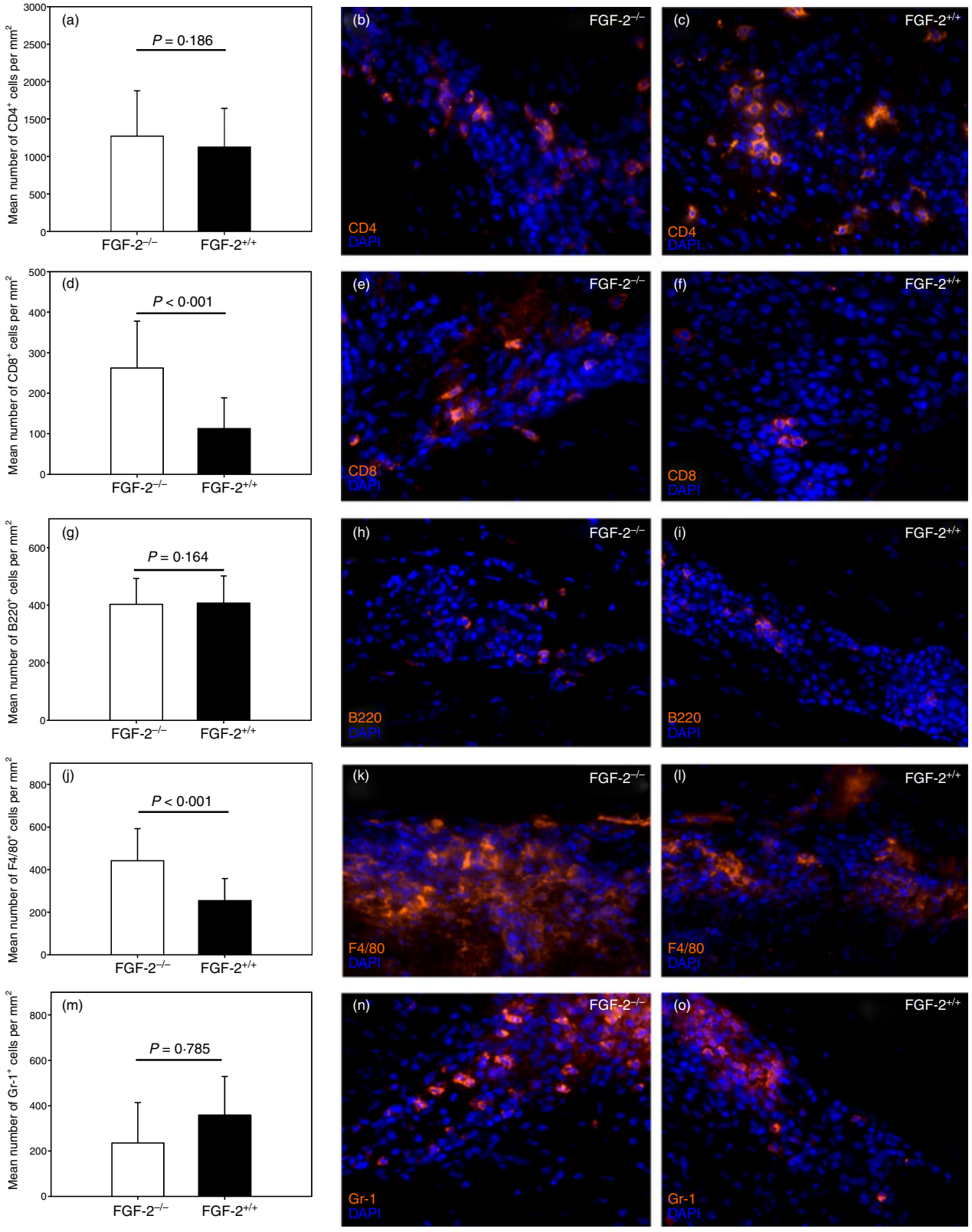

Figure 4. Central nervous system (CNS) lesion composition differs in fibroblast growth factor-2-deficient (FGF-$2^{-/-}$) and FGF-$2^{+/+}$ mice. The CNS lesion composition was evaluated at the peak of experimental autoimmune encephalitis (EAE) in $n = 6$ FGF-$2^{-/-}$ and $n = 6$ FGF-$2^{+/+}$ mice. For each group of mice the mean numbers of marker positive cells + SD and representative images are shown. All images are at 400× magnification. (a–c) $CD4^+$ T cells; (d–f) $CD8^+$ T cells; (g–i) B cells; (j–l) macrophages/microglia; (m–o) granulocytes.

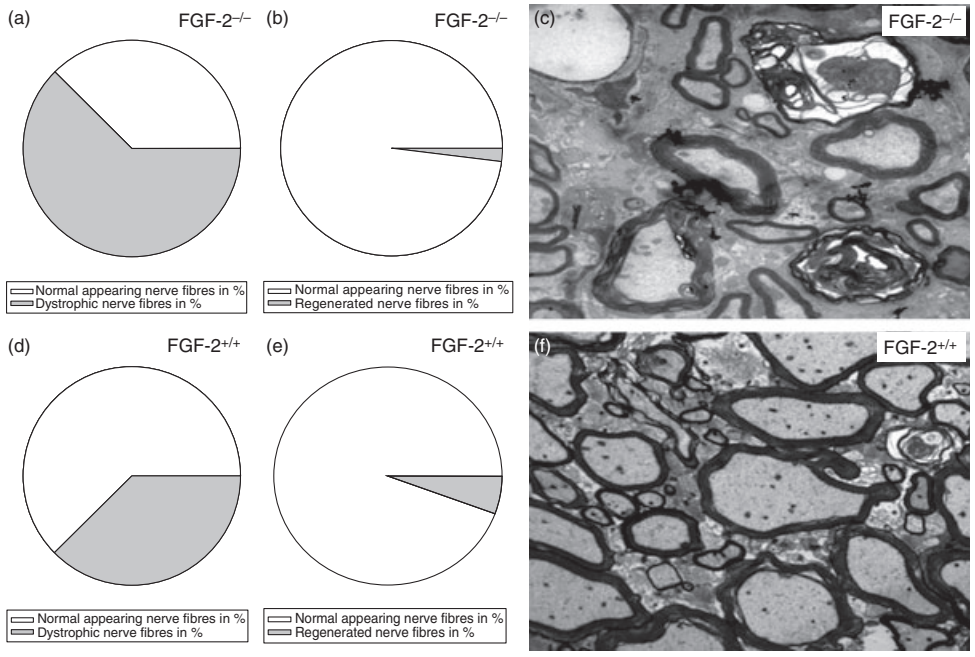

Figure 5. Central nervous system (CNS) degeneration is increased and regeneration reduced in fibroblast growth factor-2-deficient (FGF-$2^{-/-}$) compared with FGF-$2^{+/+}$ mice. The degree of nerve fibre degeneration and remyelination in CNS lesions was evaluated in FGF-$2^{-/-}$ ($n = 7$) and FGF-$2^{+/+}$ ($n = 8$) mice in chronic experimental autoimmune encephalomyelitis on day 90 after immunization with myelin oligodendrocyte glycoprotein peptide. Each nerve fibre was assessed according to the *g*-ratio (for a detailed description see Materials and methods) and categorized into either normal appearing, dystrophic or remyelinated. Degeneration included both myelin and/or axonal pathology. (a–c) The degree of nerve fibre degeneration and remyelination in FGF-$2^{-/-}$ mice including a representative electron micrograph at 3000× magnification. (d–f) The degree of nerve fibre degeneration and regeneration in FGF-$2^{+/+}$ mice including a representative electron micrograph at 3000× magnification. The results are representative of two independent experiments.

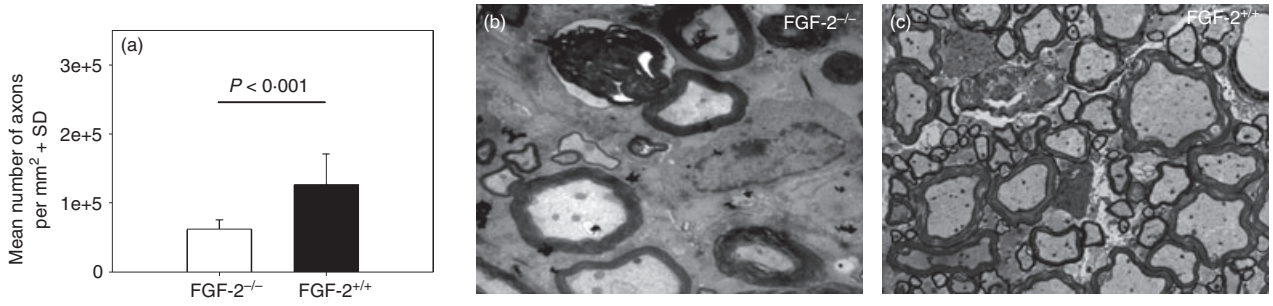

Figure 6. Axonal loss is increased in fibroblast growth factor-2-deficient (FGF-$2^{-/-}$) mice. The number of axons within central nervous system lesions was assessed in FGF-$2^{-/-}$ ($n = 7$) (a, b) and FGF-$2^{+/+}$ ($n = 8$) (a, c) mice in chronic experimental autoimmune encephalomyelitis on day 90 after immunization with myelin oligodendrocyte glycoprotein peptide. Results are shown as mean values + SD and are representative for two independent experiments. The images are electron micrographs at 3000× magnification.

contrast to 37·65 ± 16·16% in FGF-$2^{+/+}$ mice (Fig. 5a,d) ($P = 0{\cdot}011$). In FGF-$2^{-/-}$ mice we found 2·00 ± 1·11% of nerve fibres to be remyelinated, whereas in FGF-$2^{+/+}$ mice this number was significantly higher, reaching 5·59 ± 3·46% ($P = 0{\cdot}015$). Representative images are shown in Fig. 5c,f. In addition, we evaluated the magnitude of axonal loss. Figure 6 delineates that the loss of axons was significantly increased in FGF-$2^{-/-}$ (Fig. 6a,b) compared with FGF-$2^{+/+}$ mice (Fig. 6a,c) ($P = 0{\cdot}005$).

Discussion

The discussion about the involvement of growth factors in EAE/MS has intensified because it is evident that the current therapeutic strategies for the disease will not be fully successful as long as they only target the inflammatory component of the disease.[22] As disease progresses to the chronic stage, inflammation steadily decreases while degenerative features such as demyelination and axonal

damage/loss become the prime histopathological aspect of the disease.[23] The FGF-2 could be a potentially valuable agent because it has been described as supporting remyelination,[11] and reversing the clinicopathological signs of chronic EAE.[10] In the latter study, which was based upon *FGF-2* gene therapy, only single injections of a T helper : basic FGF vector showed clear beneficial effects, whereas repeated injections partially abrogated this effect. This indicates ambiguity concerning the role of FGF-2 in the disease, which is supported by other studies demonstrating that FGF-2 can impair myelinating processes.[12–14] The conflicting results delineate the necessity for further studies as to the role of FGF-2 in autoimmune encephalomyelitis and other neurodegenerative diseases.

So far there is no study making use of EAE induced in FGF-$2^{-/-}$ mice, which, with all their limitations, can be considered a clean experimental tool when it comes to assessing the systemic effects of FGF-2. Here we demonstrate significantly augmented MOG peptide 35–55-induced EAE in FGF-$2^{-/-}$ mice compared with FGF-$2^{+/+}$ mice. These differences pertained to the chronic stage of the disease whereas acute EAE was similar in both groups of mice.

There are several explanations for the differences in clinical EAE. We have previously demonstrated that brain-derived neurotrophic factor (BDNF) was crucially involved in the initiation of the peripheral immune response to the immunizing antigen.[24] BDNF$^{-/+}$ mice displayed a significantly diminished antigen-specific cytokine response and proliferation with subsequently attenuated CNS histopathology and clinical disease. This study suggested a role for growth factors beyond local mediators of pathology in the affected CNS itself. In the present study, we found the antigen-specific IFN-γ/IL-17 response to be similar in FGF-$2^{-/-}$ and FGF-$2^{+/+}$ mice. The same applied to the degree of CNS inflammation in acute and chronic EAE. However, there were differences in the lesion composition in FGF-$2^{-/-}$ and FGF-$2^{+/+}$ mice. In the former, significantly more $CD8^+$ T cells and macrophages/microglial cells were found in spinal cord infiltrates. These data may support previous results by Zechel *et al.*[9] showing a decrease of T cells and macrophages in the CNS of FGF-2-treated mice. The potential of $CD8^+$ T cells to directly mediate axonal damage has been demonstrated previously.[25–28] An increased number of macrophages/microglia could either be reflective of the need for increased CNS tissue debris removal in FGF-$2^{-/-}$ mice or rather present a pathogenic entity on its own. Macrophages/microglia are known sources of tumour necrosis factor-α and IL-1β production.[29] In particular IL-1β has been implicated in playing a crucial role in glutamate excitotoxicity, which is an established mechanism of progressive oligodendrocyte loss.[29] In addition, it has recently been discussed that microglia cells have a remarkable capacity to specifically and heterogeneously respond to changes in the healthy and injured CNS.[30–34] Fully activated microglia are known to be neurotoxic and involvement of this cell population in EAE has been previously demonstrated.[35–38] A number of molecules have been shown to be able to modulate microglial activation, including complement, antibodies, cytokines and most importantly neurotrophic factors.[35] Therefore, it is conceivable that FGF-2 can influence microglia action in MOG peptide-induced EAE. Clearly, the antibody used in this study (directed against the F4/80 molecule) does not distinguish between blood-derived macrophages and CNS-resident microglia cells. It is possible that FGF-2 has an influence on the macrophage/microglia ratio, which needs to be addressed in future studies. In addition, macrophages/microglia have been shown to secrete anti-inflammatory cytokines.[39] Lack of FGF-2 might be involved in triggering a shift from the secretion of anti-inflammatory to pro-inflammatory cytokines, which could also explain the augmented disease severity in FGF-$2^{-/-}$ mice.

In further support of an anti-inflammatory effect of FGF-2 it has been shown that CD44-mediated migration of leucocytes into the extravascular compartment could be limited by binding of FGF-2 to the CD44 receptor.[40] Also, it should be noted that FGF-$2^{-/-}$ mice displayed fluctuations in the clinical score. These fluctuations may have been reflective of immune-mediated disease relapses. In contrast, the clinical course was stable and severity was declining in FGF-$2^{+/+}$ mice. As a consequence, in the absence of relapses, the wild-type mice will have accumulated less nerve fibre damage, whereas the time for regeneration was increased relative to the FGF-$2^{-/-}$ mice. Overall, an influence of FGF-2 on the immune response cannot be eliminated and should be further evaluated in future studies.

Since differences in clinical EAE between FGF-$2^{-/-}$ and FGF-$2^{+/+}$ mice were evident in the chronic stage of EAE only, we hypothesized that FGF-2 may have particular influence on demyelination and axonal pathology, which are the histopathological hallmarks of later disease stages. Indeed, we found the degree of nerve fibre degeneration and axonal loss to be significantly increased in FGF-$2^{-/-}$ mice. At the same time the number of remyelinated axons was significantly diminished. These data implicate that the therapeutic administration of FGF-2 may need to be reconsidered as useful strategy. While Ruffini *et al.*[10] suggest only short-term administration of FGF-2 in the early phase of EAE, our data rather delineate positive effects of FGF-2 action in the chronic stage of the disease.

Our study corroborates the role of FGF-2 as a remyelinating and nerve fibre preserving agent in autoimmune encephalomyelitis. However, controversy remains as to the exact mechanism underlying this effect and the conflicting results obtained under different experimental conditions need to be carefully addressed before FGF-2 can be excluded or further considered as a therapeutic agent

for neurodegenerative diseases such as MS. Our study also shows that growth factors can act differentially. We have provided evidence for both the modulation of the peripheral immune response in the case of BDNF versus an effect primarily in the CNS itself as presented for FGF-2.

Acknowledgements

The authors express their gratitude to Mascha S. Recks and Christos Nichlos for expert technical assistance. This study was supported by grants from the Koeln Fortune Programm and the Imhoff-Stiftung to S.K.

Disclosures

The authors have no conflicts of interest to disclose.

References

1 Coles AJ, Wing MG, Molyneux P *et al.* Monoclonal antibody treatment exposes three mechanisms underlying the clinical course of multiple sclerosis. *Ann Neurol* 1999; **46**:296–304.
2 Gospodarowicz D, Moran JS. Mitogenic effect of fibroblast growth factor on early passage cultures of human and murine fibroblasts. *J Cell Biol* 1975; **66**:451–7.
3 Basilico C, Moscatelli D. The FGF family of growth factors and oncogenes. *Adv Cancer Res* 1992; **59**:115–65.
4 Palmer TD, Ray J, Gage FH. FGF-2-responsive neuronal progenitors reside in proliferative and quiescent regions of the adult rodent brain. *Mol Cell Neurosci* 1995; **6**:474–86.
5 Okabe S, Forsberg-Nilsson K, Spiro AC, Segal M, McKay RD. Development of neuronal precursor cells and functional postmitotic neurons from embryonic stem cells *in vitro*. *Mech Dev* 1996; **59**:89–102.
6 Vicario-Abejón C, Johe KK, Hazel TG, Collazo D, McKay RD. Functions of basic fibroblast growth factor and neurotrophins in the differentiation of hippocampal neurons. *Neuron* 1995; **5**:105–14.
7 Walicke PA, Baird A. Neurotrophic effects of basic and acidic fibroblast growth factors are not mediated through glial cells. *Dev Brain Res* 1998; **40**:71–9.
8 Abe K, Takayanagi M, Saito H. A comparison of neurotrophic effects of epidermal growth factor and basic fibroblast growth factor in primary cultured neurons from various regions of fetal rat brain. *Jpn J Pharmacol* 1990; **54**:45–51.
9 Zechel S, Werner S, Unsicker K, von Bohlen und Halbach O. Expression and functions of fibroblast growth factor 2 (FGF-2) in hippocampal formation. *Neuroscientist* 2010; **16**:357–73.
10 Ruffini F, Furlan R, Poliani PL *et al.* Fibroblast growth factor-II gene therapy reverts the clinical course and the pathological signs of chronic experimental autoimmune encephalomyelitis in C57BL/6 mice. *Gene Ther* 2001; **8**:1207–13.
11 Messersmith DJ, Murtie JC, Le TQ, Frost EE, Armstrong RC. Fibroblast growth factor-2 (FGF-2) and FGF receptor expression in an experimental demyelinating disease with extensive remyelination. *J Neurosci Res* 2000; **62**:241–56.
12 Goddard DR, Berry M, Kirvell SL, Butt AM. Fibroblast growth factor-2 inhibits myelin production by oligodendrocytes *in vivo*. *Mol Cell Neurosci* 2001; **18**:557–69.
13 Butt AM, Dinsdale J. Opposing actions of fibroblast growth factor-2 on early and late oligodendrocyte lineage cells *in vivo*. *J Neuroimmunol* 2005; **166**:75–87.
14 Armstrong RC, Le TQ, Flint NC, Vana AC, Zhou YX. Endogenous cell repair of chronic demyelination. *J Neuropathol Exp Neurol* 2006; **65**:245–56.
15 Sarchielli P, Di Filippo M, Ercolani MV *et al.* Fibroblast growth factor-2 levels are elevated in the cerebrospinal fluid of multiple sclerosis patients. *Neurosci Lett* 2008; **435**:223–8.
16 Zhou M, Sutliff RL, Paul RJ *et al.* Fibroblast growth factor 2 control of vascular tone. *Nat Med* 1998; **4**:201–7.
17 Kuerten S, Rodi M, Javeri S, Gruppe TL, Tary-Lehmann M, Lehmann PV, Addicks K. Delineating the impact of neuroantigen vs genetic diversity on MP4-induced EAE of C57BL/6 and B6.129 mice. *APMIS* 2009; **117**:923–35.
18 Guy J, Ellis EA, Hope GM, Emerson S. Maintenance of myelinated fibre g ratio in acute experimental allergic encephalomyelitis. *Brain* 1991; **114**:281–94.
19 Rushton WAH. A theory of the effects of fibre size in medullated nerve. *J Physiol* 1951; **115**:101–22.
20 Bishop GH, Clare MH, Landau WM. The relation of axon sheath thickness to fibre size in the central nervous system of vertebrates. *Int J Neurosci* 1971; **2**:69–77.
21 Goldman L, Albus JS. Computation of impulse conduction in myelinated fibres: theoretical basis of the velocity–diameter relation. *Biophys J* 1968; **8**:596–607.
22 Recks M, Bader J, Kaiser CC, Schroeter M, Fink GR, Addicks K, Kuerten S. Axonal damage and its importance for the concept of neurodegeneration in multiple sclerosis. *Fortschr Neurol Psychiatr* 2011; **79**:161–70.
23 Sospedra M, Martin R. Immunology of multiple sclerosis. *Annu Rev Immunol* 2005; **23**:683–747.
24 Javeri S, Rodi M, Tary-Lehmann M, Lehmann PV, Addicks K, Kuerten S. Involvement of brain-derived neurotrophic factor (BDNF) in MP4-induced autoimmune encephalomyelitis. *Clin Immunol* 2010; **137**:181–9.
25 Bitsch A, Schuschardt J, Brunkowski S, Kuhlmann T, Brück W. Acute axonal injury in multiple sclerosis. Correlation with demyelination and inflammation. *Brain* 2000; **123**:1174–83.
26 Rivera-Quiñones C, McGavern D, Schmelzer JD, Hunter SF, Low PA, Rodriguez M. Absence of neurological deficits following extensive demyelination in a class I-deficient murine model of multiple sclerosis. *Nat Med* 1998; **4**:187–93.
27 Howe CL, Adelson JD, Rodriguez M. Absence of perforin expression confers axonal protection despite demyelination. *Neurobiol Dis* 2007; **25**:354–9.
28 Medana I, Martinic MA, Wekerle H, Neumann H. Transection of major histocompatibility complex class I-induced neuritis by cytotoxic T lymphocytes. *Am J Pathol* 2001; **159**:809–15.
29 Takahashi JL, Giuliana F, Power C, Imai Y, Wee Yong V. Interleukin-1β promotes oligodendrocyte death through glutamate excitotoxicity. *Ann Neurol* 2003; **53**:588–95.
30 Hanisch UK, Kettenmann H. Microglia: active sensor and versatile effector cells in the normal and pathologic brain. *Nat Neurosci* 2007; **10**:1387–94.
31 Olah M, Biber K, Binet J, Boddeke HW. Microglia phenotype diversity. *CNS Neurol Disord Drug Targets* 2001; **10**:108–18.
32 Graber MB. Changing face of microglia. *Science* 2010; **330**:783–8.
33 Perry VH, Nicoll JA, Holmes C. Microglia in neurodegenerative disease. *Nat Rev Neurol* 2010; **6**:193–201.
34 Almolda B, Gonzalez B, Castellano B. Antigen presentation in EAE: role of microglia, macrophages and dendritic cells. *Front Biosci* 2011; **16**:1157–71.
35 de Haas AD, Boddeke HW, Biber K. Region-specific expression of immunoregulatory proteins on microglia in the healthy CNS. *Glia* 2008; **56**:888–94.
36 Becher B, Durell BG, Miga AV, Hickey WF, Noelle RJ. The clinical course of experimental autoimmune encephalomyelitis and inflammation is controlled by the expression of CD40 within the central nervous system. *J Exp Med* 2001; **193**:967–74.
37 Miller SD, Vanderlugt CL, Lenschow DJ, Pope JG, Karandikar NJ, Dal Canto MC, Bluestone JA. Blockade of CD28/B7-1 interaction prevents epitope spreading and clinical relapses of murine EAE. *Immunity* 1995; **3**:739–45.
38 Zehntner SP, Brisebois M, Tran E, Owens T, Fournier S. Constitutive expression of a costimulatory ligand on antigen-presenting cells in the nervous system drives demyelinating disease. *FASEB J* 2003; **17**:1910–2.
39 Mosser DM, Edwards JP. Exploring the full spectrum of macrophage activation. *Nat Rev Immunol* 2008; **8**:958–69.
40 Jones M, Tussey L, Athanasou N, DG. Heparan sulfate proteoglycan isoforms of the CD44 hyaluronan receptor induced in human inflammatory macrophages can function as paracrine regulators of fibroblast growth factor action. *J Biol Chem* 2000; **275**:7964–74.